

Article

An Enhanced Phase Change Material Composite for Electrical Vehicle Thermal Management

Hamidreza Behi ^{1,2,*}, Danial Karimi ^{1,2}, Mohammadreza Behi ^{3,4}, Niloufar Nargesi ⁵, Morteza Aminian ⁶, Ali Ghanbarpour ⁷, Farid Mirmohseni ⁸, Joeri Van Mierlo ^{1,2} and Maitane Berecibar ¹

¹ Research Group MOBI—Mobility, Logistics, and Automotive Technology Research Centre, Vrije Universiteit Brussel, Pleinlaan 2, 1050 Brussels, Belgium

² Flanders Make, 3001 Heverlee, Belgium

³ Institute of Photonics and Optical Science, School of Physics, The University of Sydney, Sydney, NSW 2006, Australia

⁴ METASENSE PTY LTD., 2/11 York Street, Sydney, NSW 2000, Australia

⁵ Department of Architecture, Qazvin Branch, Islamic Azad University, Qazvin 3414896818, Iran

⁶ Department of Architecture, Shahrood Branch, Islamic Azad University, Shahrood 3614773955, Iran

⁷ School of Mechanical Engineering, Babol University of Technology, Babol 4714871167, Iran

⁸ School of Chemical and Biomolecular Engineering, The University of Sydney, Sydney, NSW 2006, Australia

* Correspondence: hamidreza.behi@vub.be; Tel.: +32-(497)-296-256

Abstract: Lithium-ion (Li-ion) battery cells are influenced by high energy, reliability, and robustness. However, they produce a noticeable amount of heat during the charging and discharging process. This paper presents an optimal thermal management system (TMS) using a phase change material (PCM) and PCM-graphite for a cylindrical Li-ion battery module. The experimental results show that the maximum temperature of the module under natural convection, PCM, and PCM-graphite cooling methods reached 64.38, 40.4, and 39 °C, respectively. It was found that the temperature of the module using PCM and PCM-graphite reduced by 38% and 40%, respectively. The temperature uniformity increased by 60% and 96% using the PCM and PCM-graphite. Moreover, some numerical simulations were solved using COMSOL Multiphysics[®] for the battery module.

Keywords: phase change materials; graphite; high thermal conductivity; thermal management; electric vehicles



Citation: Behi, H.; Karimi, D.; Behi, M.; Nargesi, N.; Aminian, M.; Ghanbarpour, A.; Mirmohseni, F.; Van Mierlo, J.; Berecibar, M. An Enhanced Phase Change Material Composite for Electrical Vehicle Thermal Management. *Designs* **2022**, *6*, 70. <https://doi.org/10.3390/designs6050070>

Academic Editor: Quanqing Yu

Received: 28 July 2022

Accepted: 19 August 2022

Published: 24 August 2022

Publisher's Note: MDPI stays neutral with regard to jurisdictional claims in published maps and institutional affiliations.



Copyright: © 2022 by the authors. Licensee MDPI, Basel, Switzerland. This article is an open access article distributed under the terms and conditions of the Creative Commons Attribution (CC BY) license (<https://creativecommons.org/licenses/by/4.0/>).

1. Introduction

The traditional combustion engine has been gradually replaced by electric vehicles (EVs) and hybrid electric vehicles due to CO₂ emissions, global warming, and fossil fuel shortages. Lithium-ion (Li-ion) batteries are selected for EV energy storage due to their tremendous features like high voltage, long cycle-life, high specific energy, and low self-discharge [1,2]. Although Li-ion batteries are the ideal energy storage for EVs, they suffer a number of drawbacks, like degradation and heat generation during the charging and discharging process [3,4]. A battery thermal management system (TMS) is vital for EVs as almost 50% of EV cost returns to the battery pack [5]. In this context, some techniques, such as equivalent circuit modeling, are used for the parameter identification of Li-ion batteries to analyze their thermal response numerically [6,7]. Moreover, online data-driven techniques are employed for the health management of these batteries [8].

Different cooling systems, constituting active, passive, and hybrid systems, have been used by researchers to cool the battery module/pack in EVs [9–11]. Active cooling methods like liquid and air cooling systems use external power [12,13]. On the other hand, passive cooling methods like a heat pipe [14], phase change materials (PCM) [15], and heat sinks [16] do not use power. Hybrid cooling systems are a combination of active and passive cooling systems which need external power [17,18]. Many analyses have been presented on battery TMS to specify their effectiveness. The air cooling system is an

effortless cooling system that benefits from low cost and a simple design [19]. However, an air cooling system needs a power source and high volume [20]. This cooling system is not successful in high-current profiles and high ambient temperatures [21]. The liquid cooling system is a reliable cooling method in the application of EVs due to the high heat-transfer coefficient of liquids [22]. Nevertheless, it suffers from high cost, complex design, high energy consumption, and leakage [23]. The heat pipe cooling system is also a famous method for battery cooling [24]. However, it needs secondary cooling for the continuous process. It also suffers from a complex design, high cost, and high volume. The PCM cooling system is a successful and common method for battery cooling. It benefits from many advantages, constituting no power, uniform cooling, simple design, and low cost [25]. PCM is a material with the ability to receive or release a high amount of energy at an almost constant temperature for a specific time [26]. Nevertheless, most PCMs suffer from low thermal conductivity [22,26]. To remove such a problem, a supportive material can be added to the pure PCM to enhance its thermal conductivity. Lots of methods, like adding fins, heat pipes, aluminum and copper mesh, copper foil, and heat sinks, have been used to remove this issue [27]. Behi et al. [28] investigated the thermal performance of PCM-assisted heat pipe for electronic cooling. They found that using the heat pipe tremendously increased the cooling ability of the PCM. Behi et al. [29] experimentally and numerically studied the enhancement of PCM energy storage using heat pipe. Karimi et al. [30] designed a passive TMS using PCM for a module. They considered the functioning of the system and validated it using Simcenter AMESim[®] and COMSOL Multiphysics[®]. In a different study, they considered the effect of an aluminum grid mesh to enhance the thermal properties of the PCM. They found that the maximum temperature of the module decreased to 36 °C using the aluminum-PCM [31]. Behi et al. [32] experimentally and numerically considered the effect of PCM-assisted heat pipe for battery cooling. They found that the combination of the PCM and heat pipe could contribute to battery cooling of up to 40.7%.

However, most of the mentioned methods not only increase the volume of the cooling system but also raise its weight. Therefore, one of the best solutions for improving the thermal conductivity of pure PCMs is the addition of additive materials like graphite. Yazici [33] experimentally studied the effect of a PCM-graphite composite on the thermal management of a battery in low-temperature ambience. Behi et al. [34] considered the cooling influence of the PCM graphite on an LTO battery cell under fast discharging. They discovered that the PCM-graphite composite is a successful method for battery cooling in passive TMS. Akula and Balaji [35] designed a novel passive PCM-E-graphite cooling system for cylindrical battery cells. They found that adding the graphite has a direct effect on the cooling effect. Yazici [33] considered the effect of a PCM-graphite matrix composite on battery temperature. They found that the PCM composite, using preheating, is an effective method for battery cooling at high discharge rates. In this study, the cooling effect of PCM and PCM-graphite were considered regarding 24 cylindrical battery cells under a 1.5C discharging rate. The battery module is directly submerged in PCM and PCM-graphite to reduce the module temperature. The thermal contact resistance is removed by applying a submerged technique, which can contribute to better cooling performance. The maximum temperature of the cells and the temperature uniformity of the module were investigated experimentally and numerically. The thermal conductivity of the PCM increased using graphite, which gives a better cooling performance. The PCM-graphite composite becomes advanced via the high thermal conductivity of graphite and the high heat storage capacity of the PCM. The void between the cells is used for PCM placement, with a zero-volume increase. It was found that the temperature of the module using PCM and PCM-graphite was reduced by 38% and 40%, respectively. Moreover, the temperature uniformity of the module was increased by 60% and 96% using the PCM and PCM-graphite, respectively.

2. Experimental Test Setup

The experimental test setup in this study consisted of a cylindrical battery module (18,650 cells) with a cell nominal capacity of 2200 mAh. The module consisted of 24 cells

with every cell fixed by a cell holder, with a space of 2 mm. The module is arranged in four columns and six rows. The test setup comprises an 18,650 battery module, a PVC box, a power supply, PCM, two K-type thermocouples, a data logger, and a personal computer. The module is connected to a PEC battery tester with a ± 0.005 accuracy in order to cycle the module. The PICO USB TC-08 was chosen as a data logger to record the module temperature. In this study, the cooling effect of natural convection, PCM, and PCM-graphite was considered. Figure 1 shows the schematic and dimensions of the battery module.

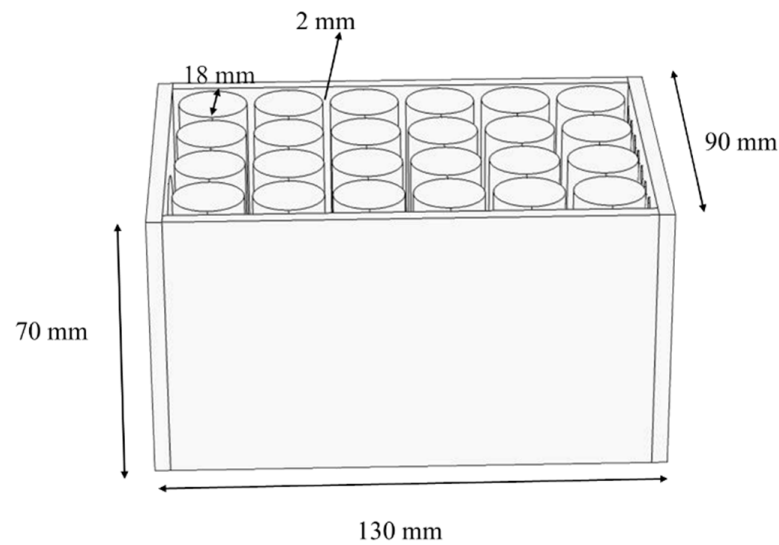


Figure 1. Schematic of the battery module with dimensions.

Cylindrical cells are structured from multiple layers of the active portion of the Li-ion battery. Therefore, there is anisotropic thermal conductivity in radial and axial directions. The important physical features of the cells applied in the battery module are shown in Table 1.

Table 1. The important physical features of the cell in the battery module are adapted from [36].

Parameters	Value	Unit
Nominal capacity	2.2	A
Nominal voltage	3.6	V
Density	2722	Kg m ⁻³
Mass	0.045	kg
Specific heat capacity	1200	J kg ⁻¹ K ⁻¹
Length	65	mm
Diameter	18	mm
Thermal conductivity	$k_r = 0.2, k_z = 37.6$ [37–40]	W m ⁻¹ K ⁻¹

In order to conduct the tests, the setup was connected to the battery tester. The module was discharged under a 1.5C rate for 2720 s. Two K-type thermocouples were linked to the cells to measure the surface temperature of the cells. The picture of the test setup and the location of the thermocouples is shown in Figure 2.

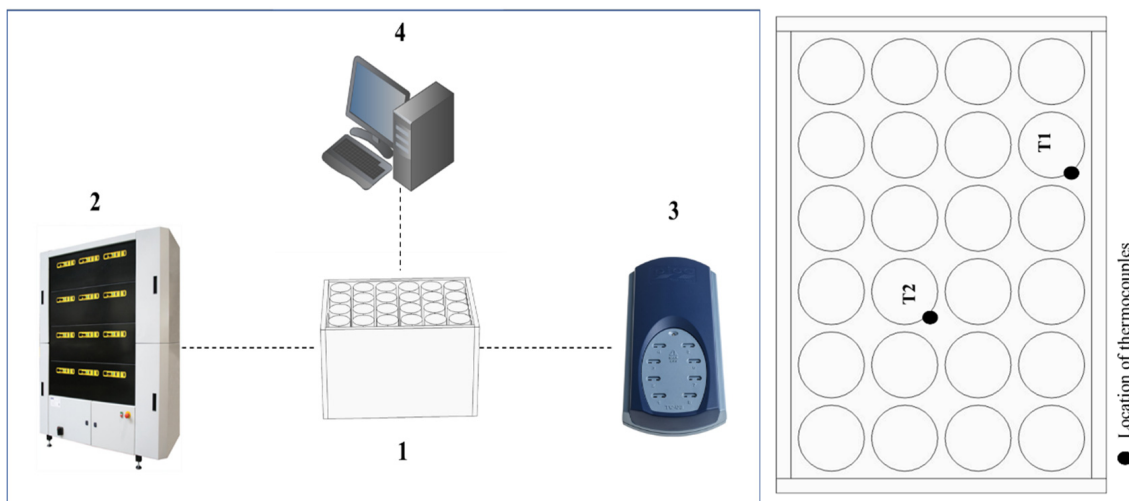


Figure 2. (left) The picture of the test setup comprising (1) the battery module, (2) battery tester, (3) data logger, (4) personal computer, (right) and the location of the thermocouples.

3. Experimental Results

3.1. Reflection of the Natural Convection

Natural convection caused by the buoyancy effect is the first cooling method that is primarily utilized to take away heat dissipation. For this reason, the surface temperature of the cells was measured under a 1.5C discharging rate. According to the data, the convection coefficient was around $6.87 \text{ W/m}^2 \text{ K}$, which was calculated experimentally [25]. Natural convection benefits from zero energy consumption, a simple design, and low cost. Figure 3 shows the temperature of the thermocouples of T_1 and T_2 under the initial temperature of $25 \text{ }^\circ\text{C}$. According to the results, the temperature of T_1 and T_2 reaches almost $57 \text{ }^\circ\text{C}$ and $65 \text{ }^\circ\text{C}$. As can be seen, there is an $8 \text{ }^\circ\text{C}$ difference between the two thermocouples, which is caused due to the location of the cells, the heat dissipation effect of other cells, and the lowered effect of natural convection in the center of the module.

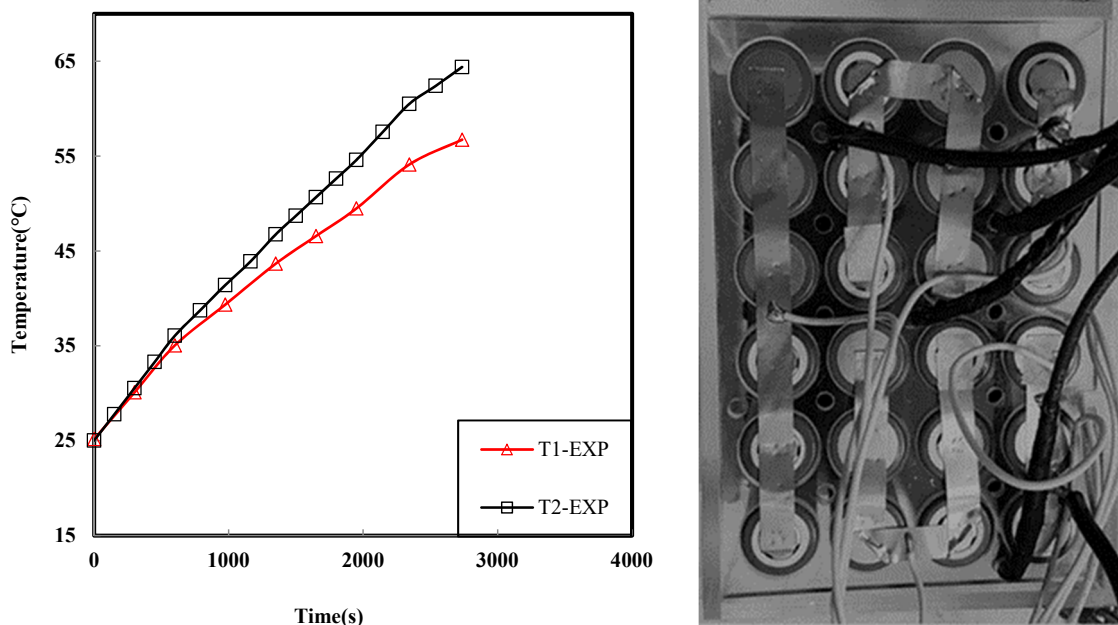


Figure 3. The temperature curve of the battery module and an image of the test setup for natural convection under a 1.5C discharging rate (EXP: Experimental).

3.2. Reflection of the PCM

PCM cooling is commonly applied as an appropriate battery thermal management method, owing to its simple design, low cost, and high performance. The PCM-based cooling system is classified as a passive cooling system, which does not need any external power source. According to the PCMs physical features, it can absorb heat at a constant temperature within the normal operating range. Therefore, based on PCM latent heat, it can keep the battery cell/module at a constant temperature for a specific time. In the current study, a paraffin PCM was used for the thermal management of the module. The PCM is classified as organic paraffin, which is produced by Shanghai Tianlan New Material Technology Co., Ltd. (Shanghai, China). The main features of the PCM are mentioned in Table 2.

Table 2. The main features of the PCM are adapted from [17].

Parameters	Value	Unit
Melting domain	35–42	°C
Max operation temperature	210	°C
Thermal conductivity (Solid-Liquid)	0.25–0.4	W/m K
Heat storage capacity	220	kJ/kg
Density (Solid-Liquid)	0.8–0.85	Kg/Lit
Specific heat capacity	2500	J/kg K

As can be seen in Figure 4, the module temperature was controlled perfectly by PCM cooling. Moreover, the temperature uniformity increased. The maximum temperature of the module reached 40.4 °C, which shows a 38% reduction compared with natural convection. There is only a 3.2 °C difference between the two thermocouples, which increased the temperature uniformity by 60%.

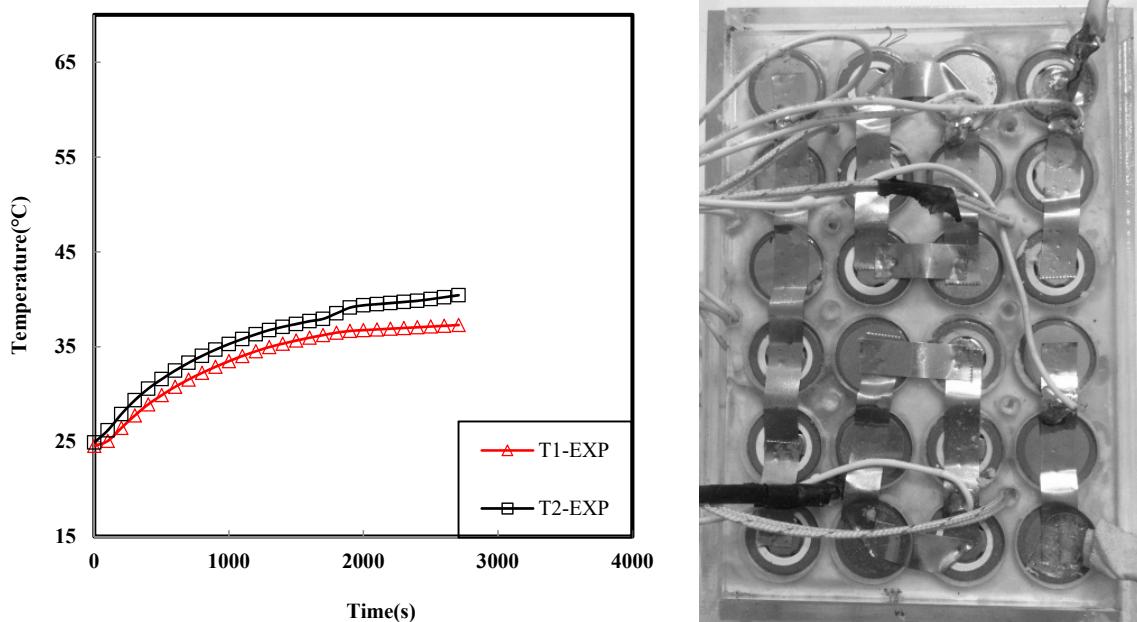


Figure 4. The temperature curve for the battery module and an image of the test setup using PCM under a 1.5C discharging rate.

Reflection of the PCM Graphite

Pure PCMs generally suffer from low thermal conductivity [7]. This drawback can be compensated for by using composite materials. Graphite, as a high thermally conductive

material, has superior advantages to increase the thermal conductivity of PCM. PCM-graphite can advance the heat conductivity of the PCM cooling system, which may increase the heat transfer efficiency. In this section, the module is in direct contact with the PCM-graphite. The main physical features of the PCM-graphite are mentioned in Table 3.

Table 3. The main features of the PCM-graphite are adapted from [17].

Parameters	Value	Unit
Melting domain	35–42	°C
Max operation temperature	210	°C
Thermal conductivity (Solid-Liquid)	0.5–1	W/m K
Heat storage capacity	210	kJ/kg
Density (Solid-Liquid)	0.8–0.85	Kg/Lit
Specific heat capacity	2500	J/kg K

Figure 5 shows the temperature curve of the battery module and a picture of the test setup using PCM-graphite. It is obvious that the module temperature has been completely controlled by the PCM-graphite. The maximum temperature of the module reached 39 °C, which shows a 40% reduction compared with natural convection. Moreover, the temperature uniformity also increased. There is only a 0.3 °C difference between the two thermocouples, which improved the temperature uniformity by 96%.

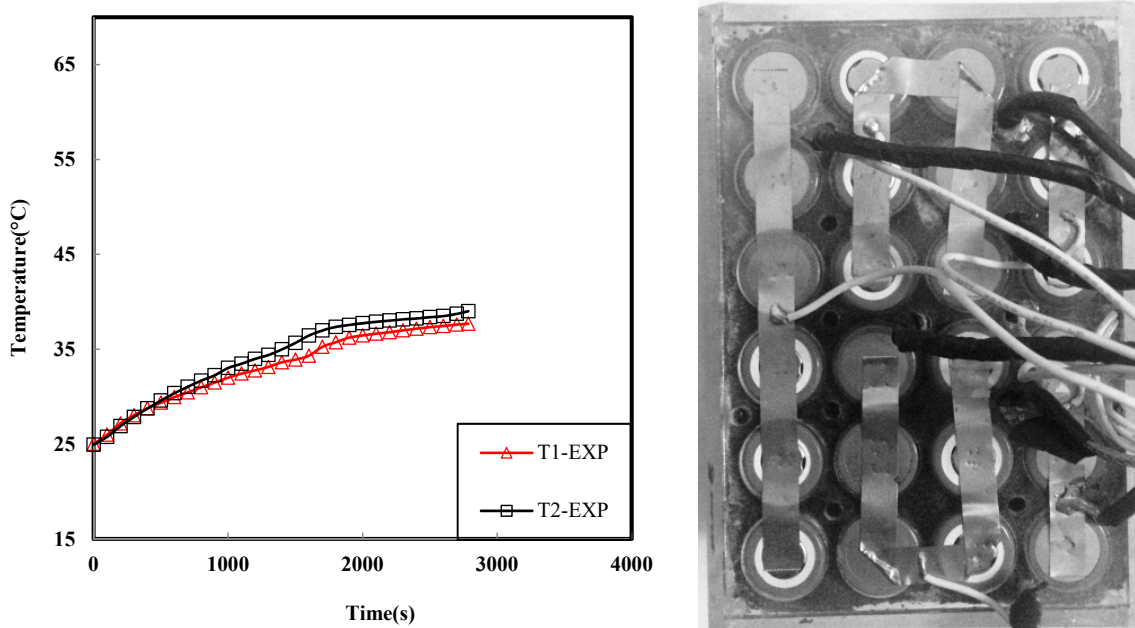


Figure 5. The temperature curve of the battery module and an image of the test setup using PCM under a 1.5C discharging rate.

3.3. Comparison of Experimental Results

The transient temperature of the T_2 thermocouple is now selected to examine the performance of the proposed cooling systems. According to the Figure 6, the temperature of T_2 reached almost 65 °C, due to the natural convection effect. This temperature is far from the acceptable Li-ion battery temperature (25–40 °C) and will definitely cause its life span to decrease. The PCM cooling systems were introduced to control the heat generation of the module. The temperature of T_2 reached 40.4 °C and 39 °C for the PCM and PCM-graphite methods, respectively. It was found that the module temperature decreased by 38% and 40% compared with natural convection, respectively.

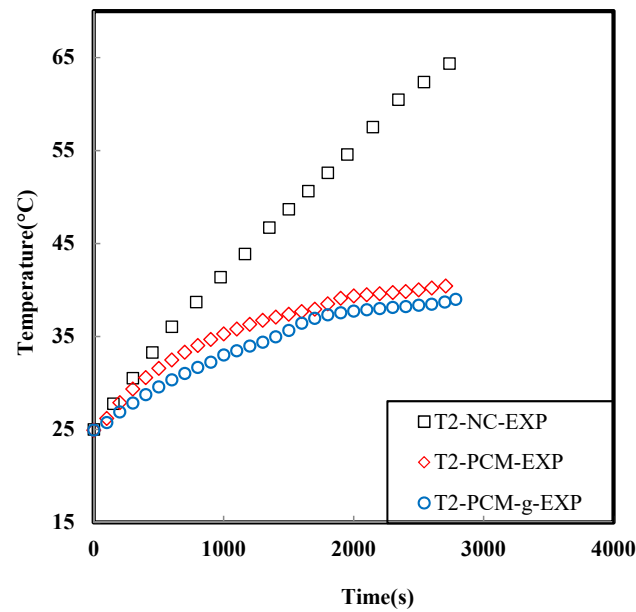


Figure 6. The comparison of the T_2 thermocouple under the different cooling technologies (NC: natural convection, PCM-g: PCM-graphite).

4. Simulation

4.1. Battery Thermal Model

In the current study, COMSOL Multiphysics® was selected to simulate the 3D thermal behavior of the cell and the PCM. The thermal model makes it possible to enhance TMS and use the battery cells in a module/pack. The internal and external resistances are the main cause of heat generation in the battery. Generally, heat generation is divided into reversible and irreversible heat. Reversible heat returns to the heat, which is generated in the cathodes and anodes and is called entropic heating. Entropic heating is produced by electrochemical reactions from reversible entropy change. It can be exothermic or endothermic based on the state of charge (SOC). The reversible battery heat generation can be calculated as follows [41]:

$$q_{rev} = I \left[T \frac{dU_{OC}}{dT} \right] \tag{1}$$

where I , T , and $\frac{dU_{OC}}{dT}$ are the current, battery temperature, and entropic heat coefficient, respectively. Irreversible heat returns to joules or ohmic heating. It can be produced due to the exchange of current within the internal resistance in the electrode, electrolyte, and current collector. The irreversible heat is always exothermic, owing to quadratic current dependence. The irreversible battery heat generation can be calculated as follows:

$$q_{irr} = I[U_{OC} - U] = RI^2 \tag{2}$$

where U_{OC} , U , and R are the open-circuit voltage, battery voltage, and the battery internal resistance, respectively. The internal resistance consists of the ohmic and polarization resistances, which depend on the SOC and battery temperature.

$$q_{gen} = q_{irr} + q_{rev} \tag{3}$$

In the present study, using a 1.5C discharge rate, a volumetric heat generation of $48,750 \text{ W/m}^3$ was selected for module simulation.

4.2. Descriptive Equations for PCM

The descriptive equations of continuity, momentum, and energy for the thermal response of the PCM are comprised as follows [7]:

$$\frac{\partial u_r}{\partial r} + \frac{u_r}{r} + \frac{\partial u_z}{\partial z} = 0 \tag{4}$$

$$\frac{\partial u_r}{\partial t} + u_r \frac{\partial u_r}{\partial r} + u_z \frac{\partial u_z}{\partial z} = -\frac{1}{\rho} \frac{\partial p}{\partial r} + \nu \left(\frac{\partial^2 u_r}{\partial r^2} + \frac{1}{r} \frac{\partial u_r}{\partial r} - \frac{u_r}{r^2} + \frac{\partial^2 u_r}{\partial z^2} \right) \tag{5}$$

$$\frac{\partial u_z}{\partial t} + u_r \frac{\partial u_z}{\partial r} + u_z \frac{\partial u_z}{\partial z} = -\frac{1}{\rho} \frac{\partial p}{\partial z} + \nu \left(\frac{\partial^2 u_z}{\partial r^2} + \frac{1}{r} \frac{\partial u_z}{\partial r} - \frac{u_r}{r^2} + \frac{\partial^2 u_z}{\partial z^2} \right) + g [\beta(T - T_m) - 1] \tag{6}$$

$$\frac{\partial h}{\partial t} + u_r \frac{\partial h}{\partial r} + u_z \frac{\partial h}{\partial z} = \frac{1}{\rho} \left[\frac{1}{r} \frac{\partial}{\partial r} \left(kr \frac{\partial T}{\partial r} \right) + \frac{\partial}{\partial z} \left(k \frac{\partial T}{\partial z} \right) \right] \tag{7}$$

In the PCM melting process, T_1 is known as an initial temperature, T_m as a melting temperature, and T_2 as a final temperature ($T_2 = T_m + \Delta T$). A mushy zone happens between the solid and liquid phases during the operation of this function within the interval of ΔT . Equation (11) shows the different phases of the PCM.

$$\begin{aligned} T^* &\leq T_1 && \text{(Solid phase)} \\ T_1 &< T^* < T_2 && \text{(Mushy phase)} \\ T^* &\geq T_2 && \text{(Liquid phase)} \end{aligned} \tag{8}$$

The heat capacity of the PCM is mentioned as a value of phase transition function, which depends on the PCM temperature (s : solid; t : transition; l : liquid):

$$C = \begin{cases} c_s & T^* \leq T_1 \\ c_t & T_1 < T^* < T_2 \\ c_l & T^* \geq T_2 \end{cases} \tag{9}$$

COMSOL, based on the defined equations, tries to simulate the heat transfer for the battery and PCM. The total amount of heat that can be received by the PCM is evaluated in the following equation:

$$Q_{PCM} = mc_s(T_1 - T_m) + mL + mc_l(T_2 - T_m) \tag{10}$$

where m is the mass of the PCM. Moreover, the thermal conductivity of the PCM can be expressed as follows:

$$C = \begin{cases} k_s & T^* \leq T_1 \\ \frac{k_s + k_l}{2} & T_1 < T^* < T_2 \\ k_l & T^* \geq T_2 \end{cases} \tag{11}$$

4.3. Validation of the Thermal Model for Natural Convection, PCM, and PCM-Graphite Cooling System

In order to validate the numerical modeling, the maximum temperature of the module (T_2) was selected to be compared with the simulation results. The simulation was conducted at a module level under the 1.5C discharging rate and at an ambient temperature of 25 °C. Figure 7 displays the validation graphs for the natural convection, PCM, and PCM-graphite cooling methods. According to the graph trends, there is an acceptable agreement between the experimental and simulation results. The root mean square error (RMSE) for natural convection, PCM and PCM-graphite cooling methods was 0.72%, 2.1%, and 1.15%, respectively.

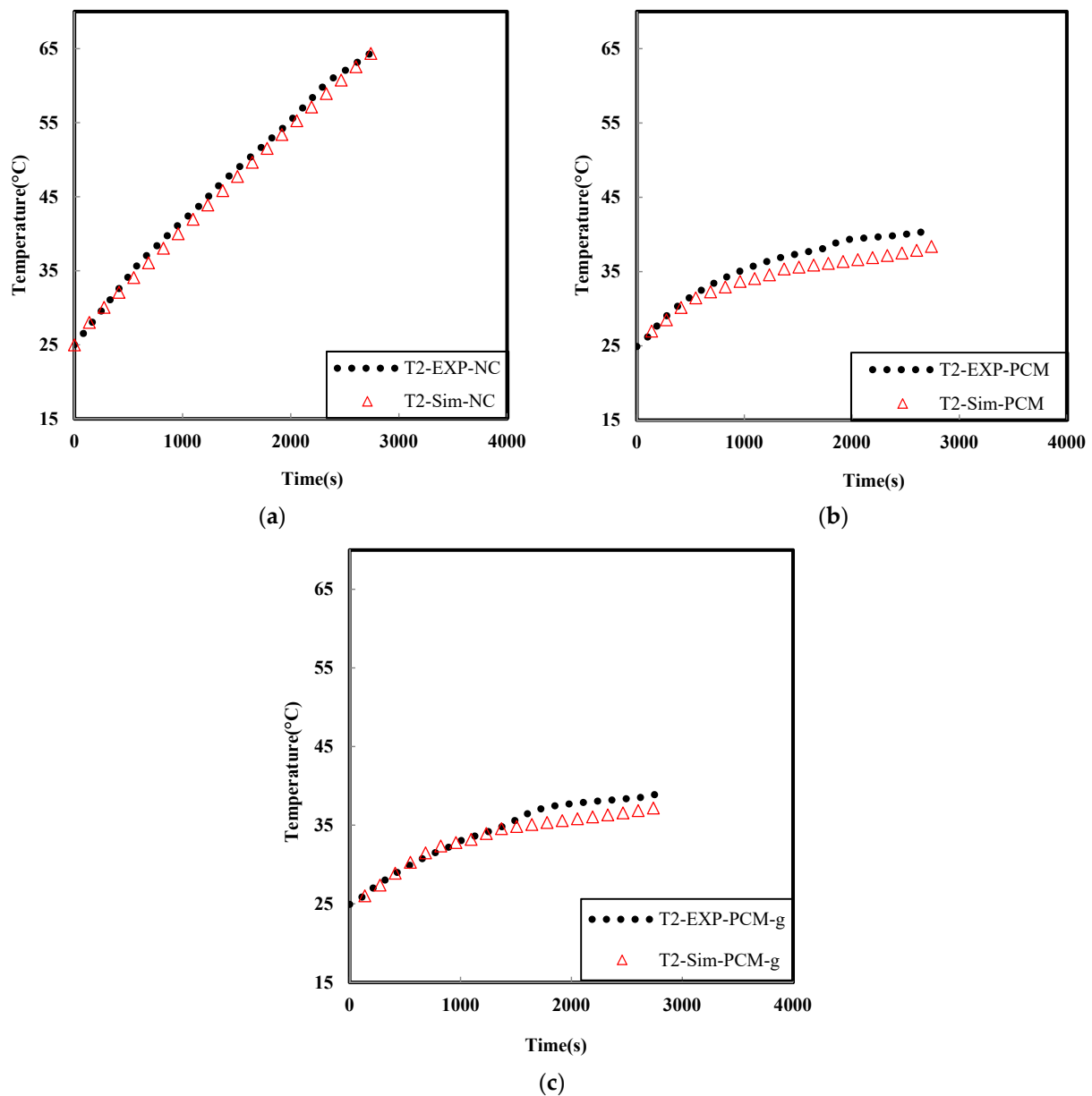


Figure 7. Thermal model validation of the module (a) under natural convection, (b) PCM, and (c) PCM-graphite at a 1.5C discharging rate (Sim: Simulation, NC: Natural convection, PCM-g: PCM-graphite).

5. Simulation Results

5.1. Thermal Behavior Contour of the Module in Different Cooling Methods

The heat transfer contour at the end of the discharging process is shown in Figure 8 (under the different cooling methods). Temperature contour is a suitable way to display the heat concentration inside the module. In natural convection cooling, the heat generation is more dominant in the center of the module due to the heat gradient of the border cells and the lower effectiveness of the free cooling. The maximum temperature reached almost 65 °C, which is outside of the safe zone for batteries. PCM cooling enacted a tremendous effect on the maximum temperature and temperature uniformity of the module. The maximum module temperature reached 40.4 °C, which proved that PCM cooling is an acceptable cooling method. In the third condition, the temperature of the module was considered under the PCM-graphite effect. It can be seen the maximum temperature reaches 38.9 °C, with more temperature uniformity, owing to the high thermal conductivity of the graphite.

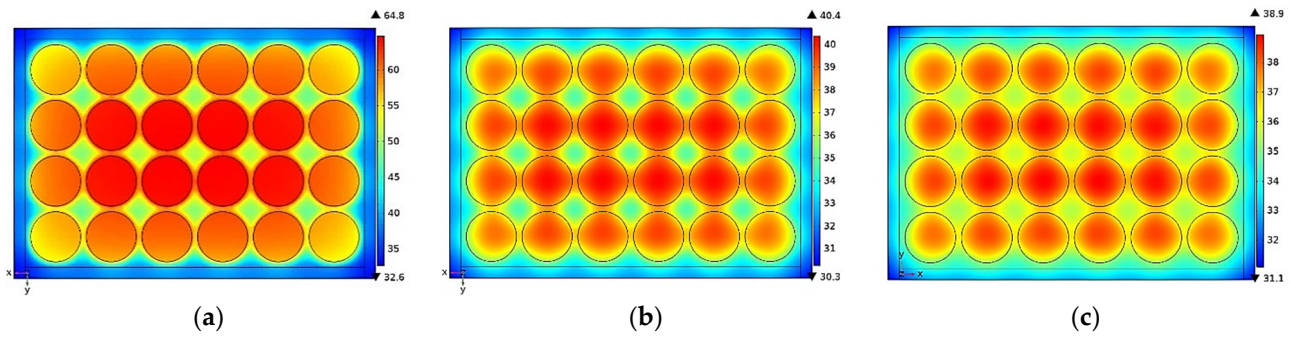


Figure 8. Temperature contour of the module using (a) natural convection (NC), (b) PCM, and (c) PCM-graphite (PCM-g) cooling methods under a 1.5C discharging rate.

5.2. Liquid Fraction Contour of Module for PCM and PCM-Graphite Cooling Methods

Figures 9 and 10 show the liquid fraction of the PCM and PCM-graphite under a 1.5C discharging process. The blue and red colors identify the solid and liquid forms of the PCM (solid = 0, liquid = 1). At the beginning of the cooling process, heat generation, along with the cells, is transferred via conduction within the PCM and PCM-graphite. In this current stage, heat is absorbed in a sensible form until it reaches the phase change temperature (mushy zone). In the mushy zone, a thin axial layer of PCM melts along the cell’s surface, as shown at 2000 s. As time passes, the melting process continues, with more heat dissipation inside the PCM (2740 s). At the phase change zone, the heat has been absorbed as a latent form and at a constant temperature. This phenomenon is the main advantage of using PCM as a cooling method. It is obvious the heat is dispersed more uniformly inside the PCM-graphite, owing to the high thermal conductivity of the graphite.

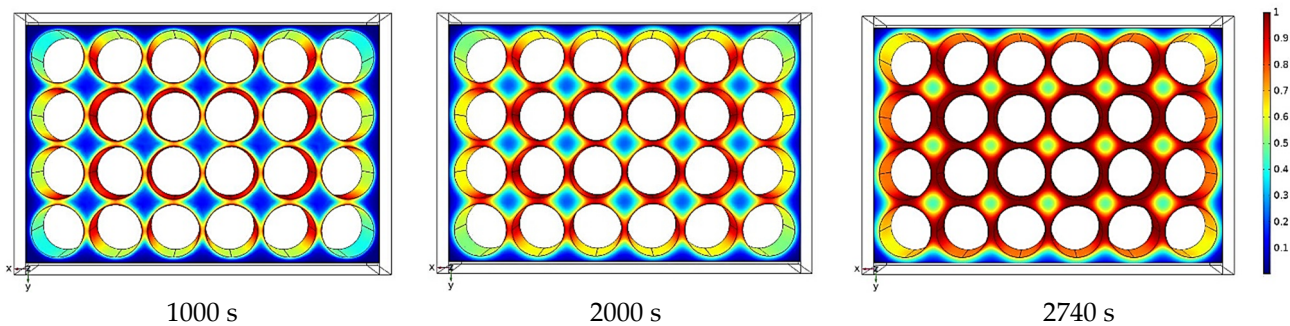


Figure 9. Liquid fraction contour of the PCM after 1000, 2000, and 2740 s under a 1.5C discharging rate.

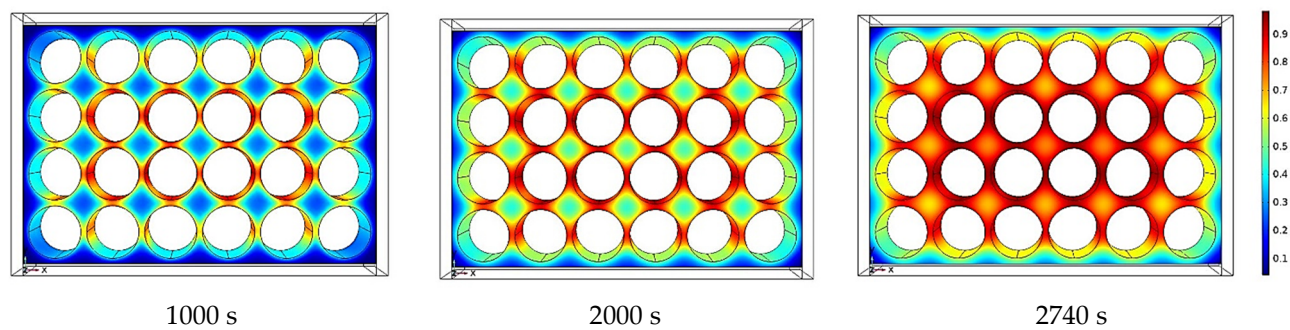


Figure 10. Liquid fraction contour of the PCM-graphite after 1000, 2000, and 2740 s under a 1.5C discharging rate.

6. Conclusions

The present study experimentally and numerically explored the cooling effectiveness of natural convection, PCM, and PCM-graphite methods for a cylindrical battery module under a 1.5C discharging rate. The results are concluded as follows:

- The maximum temperature of the module in the presence of natural convection for the initial temperature of 25 °C at a 1.5C discharging rate was measured. According to the measured results the maximum module temperature reached 64.38 °C, which is outside of the ideal Li-ion battery temperature;
- The PCM cooling system reduced the temperature of the module to 40.4 °C, which is a 38% reduction in the maximum module temperature. Moreover, the temperature uniformity of the module was increased by 60%;
- Using the PCM-graphite cooling system, the maximum module temperature reached 39 °C, which is a 40% reduction. Furthermore, the temperature uniformity of the module increased by 96%;
- The CFD model for different cooling strategies was validated against the experimental results and attained satisfactory agreement. The temperature contours and phase change process have been investigated at different times for PCM and PCM-graphite cooling systems.

Author Contributions: Conceptualization, methodology, software, validation, formal analysis, investigation, writing—original journal draft by H.B., writing, review & editing by D.K., M.B. (Mohammadreza Behi), N.N., M.A., A.G., F.M., supervision, review & editing by J.V.M. and M.B. (Maitane Berecibar). All authors have read and agreed to the published version of the manuscript.

Funding: This research received no external funding.

Institutional Review Board Statement: Not applicable.

Informed Consent Statement: Not applicable.

Data Availability Statement: Not applicable.

Conflicts of Interest: The authors declare no conflict of interest.

Nomenclature

Δt	Time Interval (t)
T	Battery Temperature (K)
I	Discharge Current (Ah)
U	Operating Voltage (V)
m	Mass of the Cell (kg)
c_p	Specific Heat Capacity (J/kg K)
q_{rev}	Reversible Heat (W)
q_{irr}	Irreversible heat (W)
R	Total Resistance of the Battery (K/W)
k	Thermal Conductivity (W/m K)
p	Pressure (Pa)
S	Cross-section of the Tab and Cell (m ²)
h	Heat Transfer Coefficient (W/m ² K)
q_{conv}	Free Cooling Heat Transfer (W)
Q_{Cell}	Power Loss of Battery (W)
ρ	Density (kg/m ³)
q_g	Cell Heat Generation (W)
V	Volume (m ³)
H	Height (m)
T_m	Melting Temperature of the PCM (K)
u	Velocity (m/s)
s	Solid Phase of PCM
l	Liquid Phase of PCM

Acronyms

CFD	Computational Fluid Dynamics
TMS	Thermal Management System
EV	Electric Vehicle
SoC	State of Charge
PCM	Phase Change Material
ESS	Energy storage system
Li-ion	Lithium-ion

References

- Kalogiannis, T.; Akbarzadeh, M.; Hosen, S.; Behi, H.; De Sutter, L.; Jin, L.; Jaguemont, J.; Van Mierlo, J.; Bercibar, M. Effects analysis on energy density optimization and thermal efficiency enhancement of the air-cooled Li-ion battery modules. *J. Energy Storage* **2022**, *48*, 103847. [\[CrossRef\]](#)
- Hosen, S.; Kalogiannis, T.; Youssef, R.; Karimi, D.; Behi, H.; Jin, L.; Van Mierlo, J.; Bercibar, M. Twin-model framework development for a comprehensive battery lifetime prediction validated with a realistic driving profile. *Energy Sci. Eng.* **2021**, *9*, 2191–2201. [\[CrossRef\]](#)
- Karimi, D.; Behi, H.; Akbarzadeh, M.; Khaleghi, S.; Van Mierlo, J.; Bercibar, M. Optimization of 1D/3D Electro-Thermal Model for Liquid-Cooled Lithium-Ion Capacitor Module in High Power Applications. *Electricity* **2021**, *2*, 503–523. [\[CrossRef\]](#)
- Karimi, D.; Behi, H.; Akbarzadeh, M.; Van Mierlo, J.; Bercibar, M. Holistic 1D Electro-Thermal Model Coupled to 3D Thermal Model for Hybrid Passive Cooling System Analysis in Electric Vehicles. *Energies* **2021**, *14*, 5924. [\[CrossRef\]](#)
- Chen, F.; Huang, R.; Wang, C.; Yu, X.; Liu, H.; Wu, Q.; Qian, K.; Bhagat, R. Air and PCM cooling for battery thermal management considering battery cycle life. *Appl. Therm. Eng.* **2020**, *173*, 115154. [\[CrossRef\]](#)
- Hosen, S.; Karimi, D.; Kalogiannis, T.; Pirooz, A.; Jaguemont, J.; Bercibar, M.; Van Mierlo, J. Electro-aging model development of nickel-manganese-cobalt lithium-ion technology validated with light and heavy-duty real-life profiles. *J. Energy Storage* **2020**, *28*, 101265. [\[CrossRef\]](#)
- Karimi, D.; Behi, H.; Van Mierlo, J.; Bercibar, M. An Experimental Study on Thermal Performance of Graphite-Based Phase-Change Materials for High-Power Batteries. *Energies* **2022**, *15*, 2515. [\[CrossRef\]](#)
- Khaleghi, S.; Hosen, S.; Karimi, D.; Behi, H.; Beheshti, S.H.; Van Mierlo, J.; Bercibar, M. Developing an online data-driven approach for prognostics and health management of lithium-ion batteries. *Appl. Energy* **2021**, *308*, 118348. [\[CrossRef\]](#)
- Karimi, D.; Behi, H.; Akbarzadeh, M.; Van Mierlo, J.; Bercibar, M. A Novel Air-Cooled Thermal Management Approach towards High-Power Lithium-Ion Capacitor Module for Electric Vehicles. *Energies* **2021**, *14*, 7150. [\[CrossRef\]](#)
- Karimi, D.; Behi, H.; Jaguemont, J.; Bercibar, M.; van Mierlo, J. A refrigerant-based thermal management system for a fast charging process for lithium-ion batteries. In Proceedings of the International Conference on Renewable Energy Systems and Environmental Engineering (IRESE2020), Brussels, Belgium, 17–18 October 2020; Global Publisher: Brussels, Belgium, 2020; pp. 1–6.
- Behi, H.; Karimi, D.; Kalogiannis, T.; He, J.; Patil, M.S.; Muller, J.-D.; Haider, A.; Van Mierlo, J.; Bercibar, M. Advanced hybrid thermal management system for LTO battery module under fast charging. *Case Stud. Therm. Eng.* **2022**, *33*, 101938. [\[CrossRef\]](#)
- Möller, S.; Karimi, D.; Vanegas, O.; el Baghdadi, M.; Kospach, A.; Lis, A.; Hegazy, O.; Abart, C.; Offenbach, A.B. Application considerations for Double Sided Cooled Modules in Automotive Environment. In Proceedings of the 11th International Conference on Integrated Power Electronics Systems, Berlin, Germany, 24–26 March 2020.
- Karimi, D.; Behi, H.; Van Mierlo, J.; Bercibar, M. A Comprehensive Review of Lithium-Ion Capacitor Technology: Theory, Development, Modeling, Thermal Management Systems, and Applications. *Molecules* **2022**, *27*, 3119. [\[CrossRef\]](#) [\[PubMed\]](#)
- Karimi, D.; Hosen, S.; Behi, H.; Khaleghi, S.; Akbarzadeh, M.; Van Mierlo, J.; Bercibar, M. A hybrid thermal management system for high power lithium-ion capacitors combining heat pipe with phase change materials. *Heliyon* **2021**, *7*, e07773. [\[CrossRef\]](#) [\[PubMed\]](#)
- Jaguemont, J.; Karimi, D.; Van Mierlo, J. Investigation of a Passive Thermal Management System for Lithium-Ion Capacitors. *IEEE Trans. Veh. Technol.* **2019**, *68*, 10518–10524. [\[CrossRef\]](#)
- Karimi, D.; Behi, H.; Jaguemont, J.; Bercibar, M.; van Mierlo, J. Investigation of extruded heat sink assisted air cooling system for lithium-ion capacitor batteries. In Proceedings of the International Conference on Renewable Energy Systems and Environmental Engineering, Brussels, Belgium, 17–18 October 2020; Global Publisher: Brussels, Belgium, 2020; pp. 1–6.
- Behi, H.; Karimi, D.; Youssef, R.; Patil, M.S.; Van Mierlo, J.; Bercibar, M. Comprehensive Passive Thermal Management Systems for Electric Vehicles. *Energies* **2021**, *14*, 3881. [\[CrossRef\]](#)
- Behi, H.; Kalogiannis, T.; Patil, M.S.; Van Mierlo, J.; Bercibar, M. A New Concept of Air Cooling and Heat Pipe for Electric Vehicles in Fast Discharging. *Energies* **2021**, *14*, 6477. [\[CrossRef\]](#)
- Karimi, D.; Behi, H.; Jaguemont, J.; Bercibar, M.; van Mierlo, J. Optimized air-cooling thermal management system for high power lithium-ion capacitors. In Proceedings of the International Conference on Renewable Energy Systems and Environmental Engineering (IRESE2020), Brussels, Belgium, 17–18 October 2020; Volume 1.

20. Akbarzadeh, M.; Kalogiannis, T.; Jaguemont, J.; Jin, L.; Behi, H.; Karimi, D.; Beheshti, H.; Van Mierlo, J.; Berecibar, M. A comparative study between air cooling and liquid cooling thermal management systems for a high-energy lithium-ion battery module. *Appl. Therm. Eng.* **2021**, *198*, 117503. [[CrossRef](#)]
21. Karimi, D.; Khaleghi, S.; Behi, H.; Beheshti, H.; Hosen, S.; Akbarzadeh, M.; Van Mierlo, J.; Berecibar, M. Lithium-Ion Capacitor Lifetime Extension through an Optimal Thermal Management System for Smart Grid Applications. *Energies* **2021**, *14*, 2907. [[CrossRef](#)]
22. Gandoman, F.H.; Behi, H.; Berecibar, M.; Jaguemont, J.; Aleem, S.H.A.; Behi, M.; Van Mierlo, J. Chapter 16—Reliability evaluation of Li-ion batteries for electric vehicles applications from the thermal perspectives. In *Uncertainties in Modern Power Systems*; Zobaa, A.F., Abdel Aleem, S.H.E., Eds.; Academic Press: Cambridge, CA, USA, 2021; pp. 563–587. [[CrossRef](#)]
23. Behi, H.; Karimi, D.; Jaguemont, J.; Gandoman, F.H.; Khaleghi, S.; Van Mierlo, J.; Berecibar, M. Aluminum Heat Sink Assisted Air-Cooling Thermal Management System for High Current Applications in Electric Vehicles. In Proceedings of the 2020 AEIT International Conference of Electrical and Electronic Technologies for Automotive (AEIT AUTOMOTIVE), Turin, Italy, 18–20 November 2020.
24. Behi, H.; Karimi, D.; Jaguemont, J.; Berecibar, M.; van Mierlo, J. Experimental study on cooling performance of flat heat pipe for lithium-ion battery at various inclination angels. *Energy Perspect* **2020**, *1*, 77–92.
25. Behi, H.; Karimi, D.; Jaguemont, J.; Gandoman, F.H.; Kalogiannis, T.; Berecibar, M.; Van Mierlo, J. Novel thermal management methods to improve the performance of the Li-ion batteries in high discharge current applications. *Energy* **2021**, *224*, 120165. [[CrossRef](#)]
26. Behi, H. Experimental and Numerical Study on Heat Pipe Assisted PCM Storage System. 2015. Available online: <http://www.diva-portal.org/smash/get/diva2:850104/FULLTEXT01.pdf> (accessed on 26 July 2022).
27. Karimi, D.; Behi, H.; Van Mierlo, J.; Berecibar, M. Advanced Thermal Management Systems for High-Power Lithium-Ion Capacitors: A Comprehensive Review. *Designs* **2022**, *6*, 53. [[CrossRef](#)]
28. Behi, H.; Ghanbarpour, M.; Behi, M. Investigation of PCM-assisted heat pipe for electronic cooling. *Appl. Therm. Eng.* **2017**, *127*, 1132–1142. [[CrossRef](#)]
29. Behi, H.; Behi, M.; Ghanbarpour, A.; Karimi, D.; Azad, A.; Ghanbarpour, M.; Behnia, M. Enhancement of the Thermal Energy Storage Using Heat-Pipe-Assisted Phase Change Material. *Energies* **2021**, *14*, 6176. [[CrossRef](#)]
30. Karimi, D.; Jaguemont, J.; Behi, H.; Berecibar, M.; van den Bossche, P.; van Mierlo, J. Passive cooling based battery thermal management using phase change materials for electric vehicles. In Proceedings of the EVS33—33rd Electric Vehicle Symposium, Portland, OR, USA, 14–17 June 2020; The Electric Drive Transportation Association (EDTA): Portland, OR, USA, 2020.
31. Karimi, D.; Behi, H.; Jaguemont, J.; Sokkeh, M.A.; Kalogiannis, T.; Hosen, S.; Berecibar, M.; Van Mierlo, J. Thermal performance enhancement of phase change material using aluminum-mesh grid foil for lithium-capacitor modules. *J. Energy Storage* **2020**, *30*, 101508. [[CrossRef](#)]
32. Behi, H.; Karimi, D.; Gandoman, F.H.; Akbarzadeh, M.; Khaleghi, S.; Kalogiannis, T.; Hosen, S.; Jaguemont, J.; Van Mierlo, J.; Berecibar, M. PCM assisted heat pipe cooling system for the thermal management of an LTO cell for high-current profiles. *Case Stud. Therm. Eng.* **2021**, *25*, 100920. [[CrossRef](#)]
33. Yazici, M.Y. The effect of a new design preheating unit integrated to graphite matrix composite with phase change battery thermal management in low-temperature environment: An experimental study. *Therm. Sci. Eng. Prog.* **2022**, *29*, 101244. [[CrossRef](#)]
34. Siddique, A.R.M.; Mahmud, S.; Van Heyst, B. A comprehensive review on a passive (phase change materials) and an active (thermoelectric cooler) battery thermal management system and their limitations. *J. Power Sources* **2018**, *401*, 224–237. [[CrossRef](#)]
35. Akula, R.; Balaji, C. Thermal management of 18650 Li-ion battery using novel fins-PCM-EG composite heat sinks. *Appl. Energy* **2022**, *316*, 119048. [[CrossRef](#)]
36. Behi, H.; Karimi, D.; Behi, M.; Ghanbarpour, M.; Jaguemont, J.; Sokkeh, M.A.; Gandoman, F.H.; Berecibar, M.; Van Mierlo, J. A new concept of thermal management system in Li-ion battery using air cooling and heat pipe for electric vehicles. *Appl. Therm. Eng.* **2020**, *174*, 115280. [[CrossRef](#)]
37. Drake, S.; Wetz, D.; Ostanek, J.; Miller, S.; Heinzl, J.; Jain, A. Measurement of anisotropic thermophysical properties of cylindrical Li-ion cells. *J. Power Sources* **2014**, *252*, 298–304. [[CrossRef](#)]
38. Saw, L.; Ye, Y.; Tay, A. Electrochemical–thermal analysis of 18650 Lithium Iron Phosphate cell. *Energy Convers. Manag.* **2013**, *75*, 162–174. [[CrossRef](#)]
39. Spinner, N.S.; Hinnant, K.M.; Mazurick, R.; Brandon, A.; Rose-Pehrsson, S.L.; Tuttle, S.G. Novel 18650 lithium-ion battery surrogate cell design with anisotropic thermophysical properties for studying failure events. *J. Power Sources* **2016**, *312*, 1–11. [[CrossRef](#)]
40. Jiaqiang, E.; Yue, M.; Chen, J.; Zhu, H.; Deng, Y.; Zhu, Y.; Zhang, F.; Wen, M.; Zhang, B.; Kang, S. Effects of the different air cooling strategies on cooling performance of a lithium-ion battery module with baffle. *Appl. Therm. Eng.* **2018**, *144*, 231–241. [[CrossRef](#)]
41. Karimi, D.; Berecibar, M.; van Mierlo, J. Modular Methodology for Developing Comprehensive Active and Passive Thermal Management Systems for Electric Vehicles. Ph.D. Thesis, Vrije Universiteit Brussel, Brussels, Belgium, 2022.